Computers, Environment and Urban Systems xxx (xxxx) xxx-xxx

Contents lists available at ScienceDirect

Computers, Environment and Urban Systems

journal homepage: http://ees.elsevier.com

Integrating a Forward Feature Selection algorithm, Random Forest, and Cellular Automata to extrapolate urban growth in the Tehran-Karaj Region of Iran

Hossein Shafizadeh-Moghadam In affiliation, change from "Engineering" to "Engineering and Management"[a], Masoud Minaei[b],
Robert Gilmore Pontius Jr Eliminate comma between Pontius and Jr in name, also change from period to comma after University in affiliation, also change from Pontius to Pontius Jr where you list email addresses[c,*],

Ali Asghari Change affiliation to The Centre for Spatial Data Infrastructures and Land Administration, Department of Infrastructure Engineering, The University of Melbourne, VIC 3010, Australia[d],
Hashem Dadashpoor[e]

[a] *Department of Water Resources Engineering, Tarbiat Modares University, PO Box 14115-336, Tehran, Iran*
[b] *Department of Geography, Ferdowsi University of Mashhad, PO Box 9177948974, Mashhad, Iran*
[c] *Graduate School of Geography, Clark University. 950 Main Street, Worcester, MA 01610, USA*
[d] *Department of Infrastructure Engineering, The Centre for Spatial Data Infrastructures and Land Administration, The University of Melbourne, VIC 3010, Australia*
[e] *Department of Urban and Regional Planning, Faculty of Arts and Architecture, Tarbiat Modares University, PO Box 14115-111, Tehran, Iran*

ARTICLE INFO

Keywords
Cellular automata
Land use and land cover change
Random Forest
Raster data modeling
Urban agglomeration

ABSTRACT

This paper couples a Forward Feature Selection algorithm with Random Forest (FFS-RF) to create a transition index map, which then guides the spatial allocation for the extrapolation of urban growth using a Cellular Automata model. We used Landsat imagery to generate land cover maps at the years 1998, 2008, and 2018 for the Tehran-Karaj Region (TKR) in Iran. The FFS-RF considered the independent variables of slope, altitude, and distances from urban, crop, greenery, barren, and roads. The FFS-RF revealed temporal non-stationary of drivers from 1998–2008 to 2008–2018. The FFS-RF detected that altitude and distance from greenery were the most important drivers of urban growth during 1998–2008, then distances from crop and barren were the most important drivers during 2008–2018. We used the Total Operating Characteristic to evaluate the transition index maps. Validation during 2008–2018 showed that FFS-RF produced a transition index map that had predictive power no better than an allocation of urban growth near existing urban. Simulation to 2060 extrapolated that Tehran, Karaj, and their adjacent cities will interconnect spatially to form a gigantic city-region.

1. Introduction

A great deal of literature exists concerning the simulation of urban growth for various cities around the globe (Gounaridis, Chorianopoulos, Symeonakis, & Koukoulas, 2019; Pontius Jr et al., 2018; Rafiee, Mahiny, Khorasani, Darvishsefat, & Danekar, 2009; Wang, Derdouri, & Murayama, 2018). These simulations require an understanding of the growth patterns and their driving forces (Paegelow, Camacho Olmedo, Houet, Mas, & Pontius Jr, 2013). Identifying the main forces is a formidable challenge due to the plethora of possible urban growth drivers. The main objectives of this paper are to rank independent variables according to their association with urban growth during calibration and validation time intervals, and then to extrapolate urban growth over decades in Iran's Tehran-Karaj region.

The urban growth pattern is a function of various drivers such as socioeconomic issues, environmental factors, and policy options, which can operate intricately. Therefore, a diverse spectrum of growth patterns from compact to sprawling might occur. One of the important forms of urbanization is urban agglomeration, which is a phenomenon that Geddes (1915) predicted to be the future trend of urbanization. Studies on the spatial agglomeration of cities began as early as the 1920s, with various terms used to describe this particular urban spatial

* Corresponding author.
E-mail addresses: h_shafizadeh@modares.ac.ir (H. Shafizadeh-Moghadam); m.minaei@um.ac.ir (M. Minaei); rpontius@clarku.edu (R.G. Pontius); aasghari@student.unimelb.edu.au (A. Asghari); H-dadashpoor@modares.ac.ir (H. Dadashpoor)

https://doi.org/10.1016/j.compenvurbsys.2021.101595
Received 18 June 2020; Received in revised form 29 November 2020; Accepted 7 January 2021
Available online xxx

organization. A clear definition of urban agglomeration is still up for debate and researchers have proposed a variety of terms (Howard, 1902). Literature frequently uses the term "urban agglomeration", while other popular synonyms are city clusters, city group, and megalopolis. Urban agglomeration appears as a result of cooperation and competition among cities (Fang & Yu, 2017). Urban agglomeration refers to the extensive continuous expansion of urban areas. In other words, an urban agglomeration is the result of the coalescence of adjacent cities (Zhang et al., 2019). This phenomenon has been unprecedentedly increasing at the global level. The importance of urban clusters was reflected in the work of Fang and Yu (2017) who reported that the study of urban clusters increased from very few publications as of 1952 to over thirty-two thousand publications as of 2015. Fast-growing urban agglomeration can affect the sustainability of urban areas (Zhang et al., 2019). For example, urban agglomeration has threatened regional ecotopes and changed ecosystem structures and ecological landscapes (Zhou, Huang, Yu, & Wang, 2015). Therefore, the detection of emerging urban agglomerations and understanding their underlying drivers is critical. Urban agglomerations have been extensively studied in Asia (Wei, Taubenböck, & Blaschke, 2017; Zhang et al., 2019), while less attention has been paid to emerging urban clusters in Iran.

Iran is the 17th most populous country in the world with a population of more than 79 million in 2016 (Statistical Center of Iran, 2016). On a global scale, Iran has one of the highest urbanization rates, which is mainly attributed to population growth, economic growth, and internal migration from rural areas due to inequalities and social differences (Fanni, 2006). The distribution of Iranian cities shows an unbalanced spatial arrangement with vast areas of low urbanization density and some very congested areas. The patterns of urban growth in densely populated areas and their impact on their surrounding landscapes are problems that have been insufficiently studied. The Tehran-Karaj Region (TKR) is a large urban area in Iran consisting of Tehran, Iran's capital, and nearby Karaj, the capital of Alborz province. TKR comprises a cluster of small and large cities that are growing exponentially and are spatially amalgamated (Shafizadeh-Moghadam, 2019). The region faces extensive immigration from various parts of Iran, which is due to the concentration in TKR of industrial activities, service occupations, recreational amenities, welfare facilities, and health services. These conditions have caused unbridled development of the TKR that originates from the lack of spatial justice in the Iranian cities, which is a problem that has exacerbated the population imbalance in the country. The intensity of migration to the TKR has led to a sharp decline in gardens and croplands, which transitioned to urban areas. This process has caused many urban fringes over time. Simultaneously, neighboring counties have evolved so that the contemporary urban areas cover a densely populated TKR. Still, the construction process in the TKR is uninterruptedly on-going; hence, simulation of the future pattern of urban growth in the TKR can inform urban planning, environmental management, and mitigation strategy.

Currently, it is feasible to discover the emerging urban clusters and envisage their spatial patterns by using spatial models that consider satellite imageries. Remote sensing data, in particular Landsat images, are of great importance in providing a spatiotemporal footprint of urban areas and mapping land cover (Minaei & Kainz, 2016). Hence, we adopt the Landsat time series to track retrospective land changes in the TKR and to provide data to simulate the future pattern of growth in this region. Several models have been developed to connect urban changes with underlying driving forces, for example, Random Forest (RF) (Gounaridis et al., 2019; Kamusoko & Gamba, 2015), Artificial Neural Networks (Pijanowski, Brown, Shellito, & Manik, 2002; Tayyebi & Pijanowski, 2014), Logistic Regression (Feng, Liu, & Liu, 2017; Lin, Chu, Wu, & Verburg, 2011), and Support Vector Machine (Rienow & Goetzke, 2015; Shafizadeh-Moghadam, Asghari, Tayyebi, & Taleai, 2017). Also, Moulds, Buytaert, and Mijic (2015) developed an open-source package for modeling land change through a variety of spatial models. Recognizing the relevant drivers of change for these models is not straightforward because drivers can include redundant variables that interact in complex ways. Identifying and ignoring non-informative variables from the modeling process is thus critical (Kuhn & Johnson, 2013). The RF model is appealing because RF is an approach that accounts for variable interactions, handles complex relationships, and extracts variable importance. Feature selection can increase the model fit considerably (Meyer, Reudenbach, Hengl, Katurji, & Nauss, 2018). In our study, we apply an RF model with a feature selection approach to rank urbanization forces and to simulate the trajectories of urban growth over time.

2. Data and methods

2.1. Study area

This paper focuses on two adjacent megacities, namely Tehran and Karaj, and several cities around them. Until 2010, Tehran and Karaj belonged to the same province and since then, Karaj has been the capital of Iran's Alborz province. Both cities and their surrounding settlements are highly intertwined. Fig. 1 shows the TKR in the south of the Alborz mountain range. Tehran (35° 41′ N and 51° 23′E) is the largest urban region in Iran, while Karaj (35°50′ N, 50°56′ E) is the fourth largest. The population of the metropolitan areas of Tehran and Karaj is approximately 13 and 3 million, respectively (Statistical Center of Iran, 2016). TKR has 850 people per square km, which is 17 times higher than the national average.

The trend of growth and urban expansion in agricultural areas south of Tehran's metropolitan area, along the Karaj River and the Varamin plain, leads to the conversion of several thousand villages into small, intermediate, and large cities (Habibi & Horcad, 2005). Rural areas located along the main road networks near Tehran with inexpensive land and weak regulation have a high potential to become urbanized. Flatlands, hills, mountains, and riversides are under construction. Fig. 2 shows a planned development. Physical restrictions cause urban growth in the northern parts of TKR to be less than in other parts.

Housing has become a major problem in most megacities of Iran, particularly in Tehran and Karaj. The development of new cities has been on the agenda to prevent the unbridled growth of existing cities and to decentralize the population. Several new cities have been created during the last two decades, for example, Pardis 30 km east of Tehran, Andisheh 20 km west of Tehran, and Hashtgerd northwest Karaj. Our article considers a $\sim$ 7600 square km spatial extent, including Karaj and its adjacent counties, including Fardis, Hashtgerds, and Nazarabad, as well as Tehran and its nearby counties including Pakdasht, Varamin, Eslamshahr, Robatkarim, Shahr-e-Rey, and Shahriar.

2.2. Data preparation

Landsat images of TM (May 1988), ETM^{+} (May 2008), and OLI (April 2018) are our main sources of data. All maps were projected to UTM zone 39 with a spatial resolution of 30 by 30 m. We used an RF model to classify the pixels then modified the maps based on expert knowledge and a majority filter to amalgamate isolated cells. Fig. 3 shows the maps of five land cover categories. Topographic maps, aerial photos, and Google Earth served for error assessment, which measured urban's omission error intensity and commission error intensity. Omission error intensity is the size of true urban that the map fails to show as urban divided by the size of true urban. Commission error intensity is the size of mapped urban that is truly non-urban divided by the size of mapped urban. Omission error intensities and commission error intensities were respectively 0% and 8% at 1998, 9% and 4% at 2008, and 9% and 5% at 2018. Loss of urban during 1998–2018 is negligible,

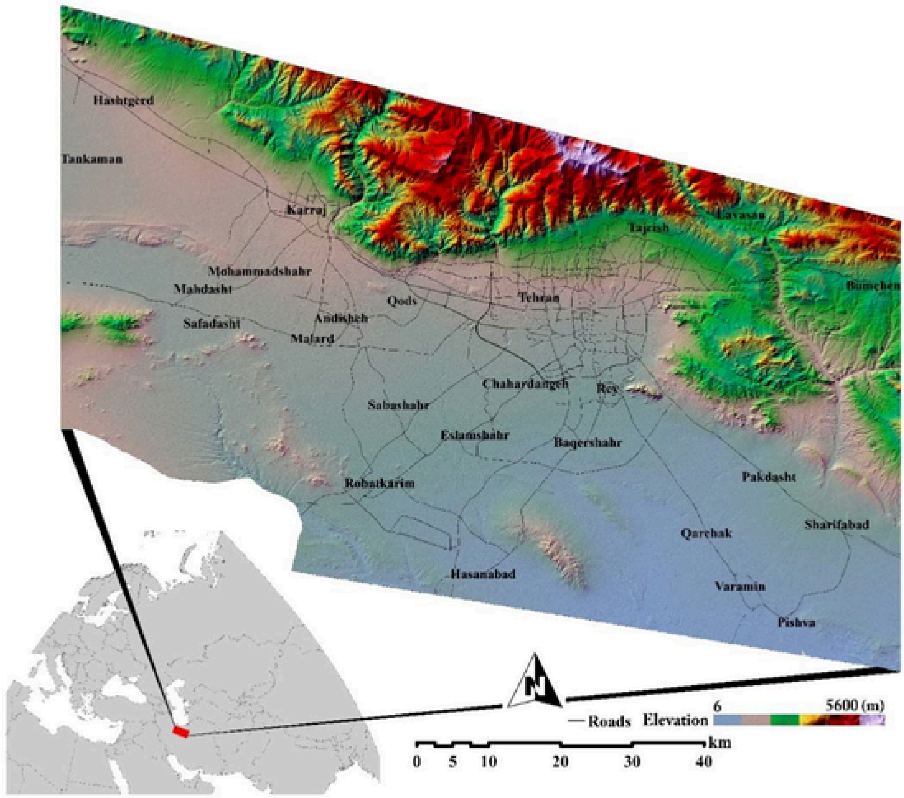

Fig. 1. Location of the study area shown on elevation.

Fig. 2. A new planned city, Pardis, to the east of Tehran. Source is www.mehrnews.com

therefore Fig. 4 shows the urban growth but not urban loss. Urban growth during 1998–2008 and 2008–2018 was 140% and 74% of the size of urban at the start of the respective decade. Our research considered seven independent variables, based on knowledge of the driving forces in the study area (Hu & Lo, 2007; Shafizadeh-Moghadam et al., 2017). Fig. 5 shows maps of the independent variables as slope, altitude, and distance from a feature at the start of the time interval. We include the distance from urban, crop, greenery, barren, and roads. Road networks of 1998 and 2008 were acquired using digitization of satellite data and high-resolution imagery. The 2018 roads layer was obtained from the OpenStreetMap. Exclusionary zones are places where urban growth is not possible due to land cover or legal restrictions (Pijanowski et al., 2002). At the beginning of each time interval, exclusionary zones consist of water bodies and greenery, which includes public parks and other green spaces. To improve the numerical stability of some calculations, we standardized each independent variable by subtracting its mean and dividing by its standard deviation (Kuhn & Johnson, 2013).

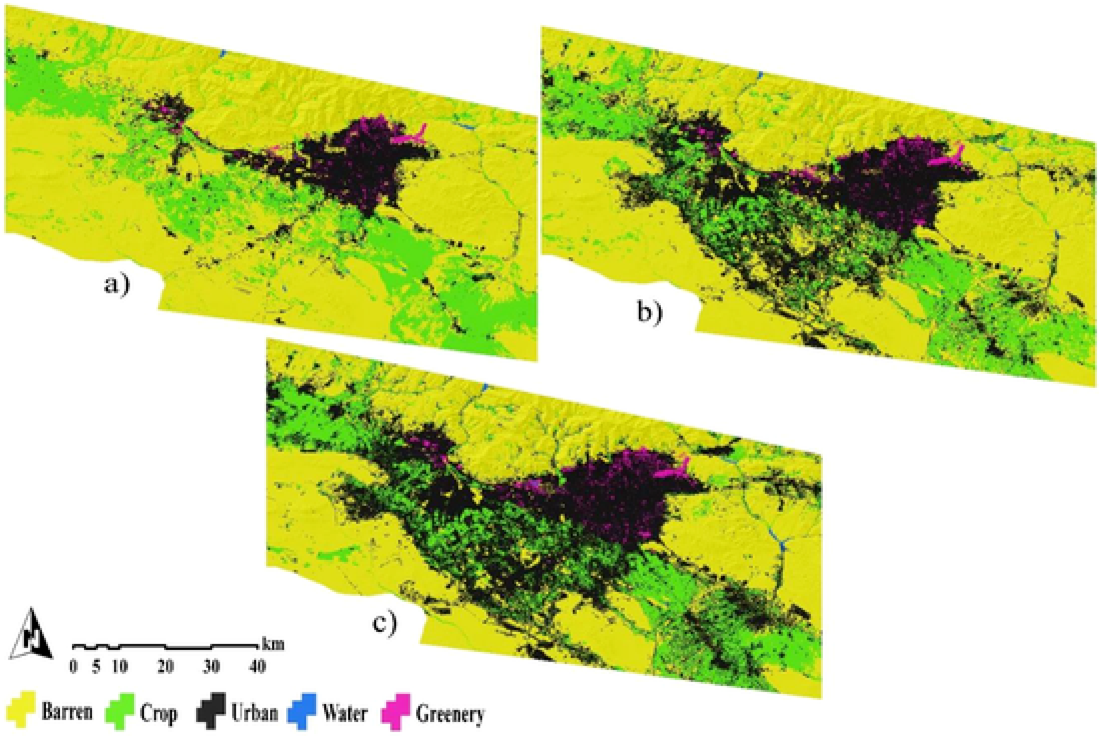

Fig. 3. Land cover maps of the Tehran-Karaj Region at a) 1998, b) 2008, and c) 2018.

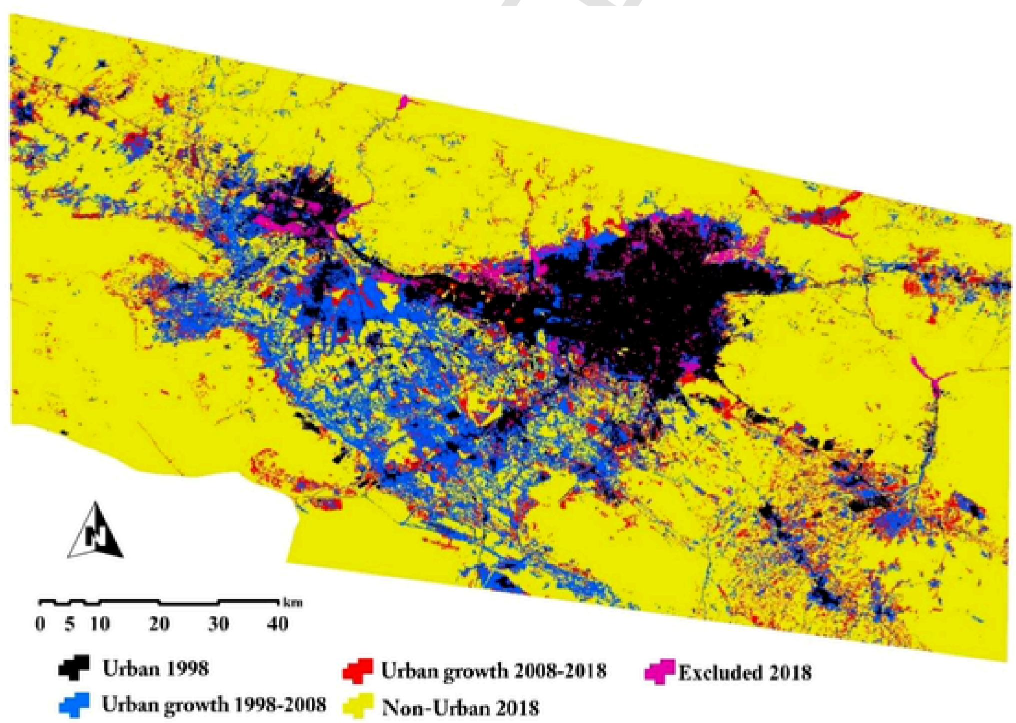

Fig. 4. Urban growth during 1998–2008 and 2008–2018 in the Tehran-Karaj Region.

2.3. Methods

2.3.1. Flow of methods

Fig. 6 is a flowchart of our methods. We performed two runs of an RF model. The first run was for calibration based on independent variables at 1998 and urban growth during 1998–2008. This first run fitted a transition index map (TIM), where higher index values show greater transition potential for urban growth after 1998 according to the fitted RF model. We used the Total Operating Characteristic (TOC) to evaluate the fit of the calibration (Pontius Jr & Si, 2014). TOC compared the calibrated fit to the fit of a baseline that has larger index values closer to urban at 1998. The calibrated TIM was then updated using independent variables at 2008 to extrapolate urban growth during

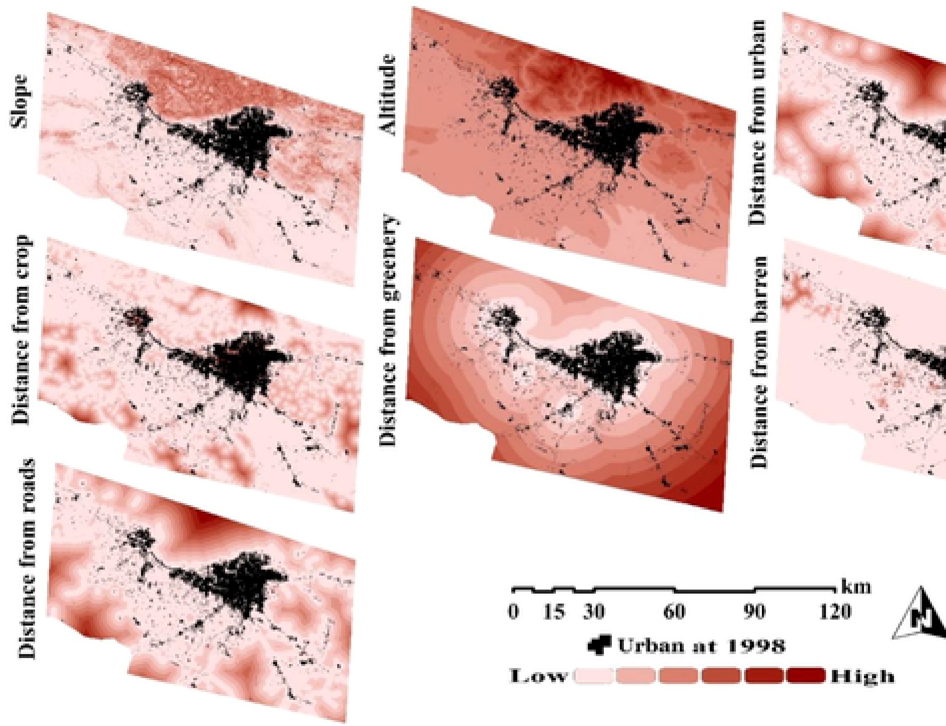

Fig. 5. Independent variables at 1998 for model calibration.

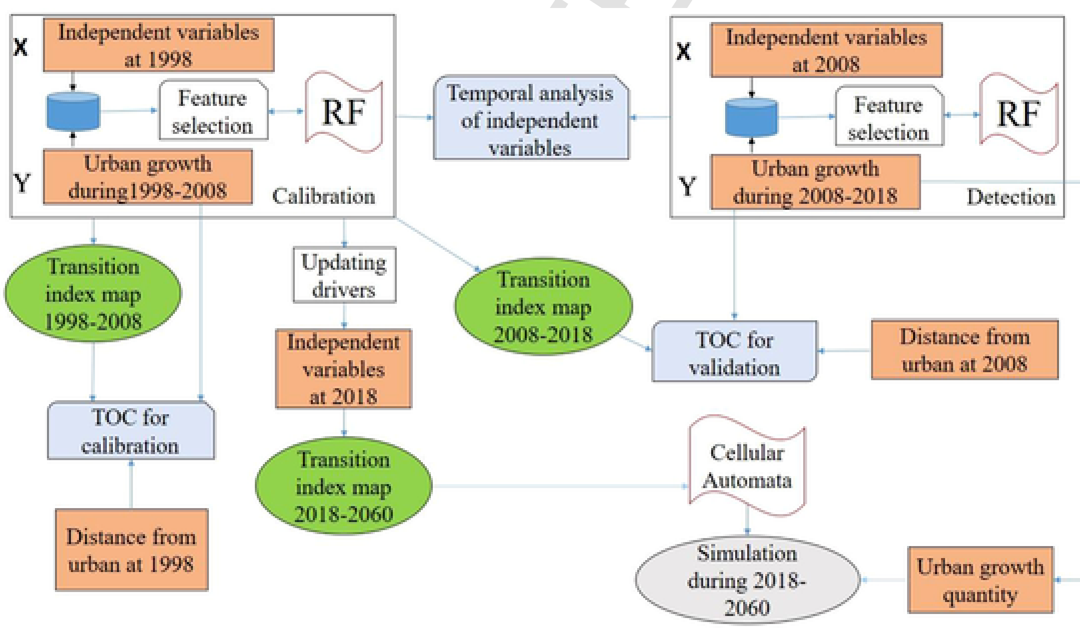

Fig. 6. Urban growth modeling flowchart.

2008–2018. We used TOC to validate the predictive power of the extrapolation during 2008–2018 and to compare its power to the power of a baseline that has larger index values closer to urban at 2008. The TIM that was calibrated for 1998–2008 was updated again using independent variables at 2018 to extrapolate urban growth during 2018–2060. Cellular Automata (CA) was applied with the TIMs to allocate the cells for the extrapolated urban growth during 2018–2060. The flowchart shows this step as the simulation during 2018–2060.

The second run of the RF model analyzes the independent variables during 2008–2018. The second RF run fitted a relationship between the independent variables at 2008 and the urban growth during 2008–2018. We performed this second run to see how the fitted relationship during 2008–2018 compares to the first run during 1998–2008. The comparison examines the stationary of urban growth factors to reveal whether the urban growth drivers during 1998–2008 are the same as during 2008–2018. The flowchart shows this comparison as the box labeled "Temporal analysis of independent variables".

2.3.2. Network plot and density plot

We created a network plot to explore the collinearity between pairs of explanatory factors. A network plot shows the correlation between pairs of explanatory variables in which more correlated pairs appear closer together and linked by thicker paths. Multidimensional clustering determines the proximity of the variables within the plot. Additionally, we created a density plot to visualize the distribution of urban growth in relation to the independent variables at the beginning of each time interval. A density plot is an empirical probability density as a function of the independent variable, for example distance from urban.

2.3.3. Forward Feature Selection – Random Forest (FFS-RF)

Random Forest (RF) is a supervised data-driven algorithm made of the reimplementation of a base learner called classification and regression tree (Breiman, 2001). We use RF to regress a binary dependent variable that distinguishes urban growth from non-urban persistence versus independent variables, for example, distance from initial urban. RF is prone to the rise of model complexity as the number of independent variables increases (Brennan, Tri, & Marcot, 2019). To alleviate the complexity, the Forward Feature Selection (FSS) algorithm selects relevant independent variables, which helps to decrease model complexity and to facilitate interpretation. In our paper, FFS was integrated with the RF (Meyer et al., 2018). FFS uses a subset of independent variables to train the model. The FFS re-implements the RF model many times, which depends on the number of independent variables (Meyer et al., 2018). Initially, the number of iterations is identical to the number of possible unique pairs of independent variables. In each iteration, the RF is implemented and the fitted value is stored. The fit is the ratio of the number of correctly fitted urban growth pixels to the total number of reference urban growth pixels. Then, a pair of independent variables that yield the best fit is selected and other variables are consequently added to the model. This process continues as long as adding new variables improves the fit. Thus, the independent variables that collectively account for the highest possible fit are selected for inclusion in the final model, which then produces a Transition Index Map (TIM).

To avoid spatial overfitting (Valavi, Elith, Lahoz-Monfort, & Guillera-Arroita, 2018), a target-oriented approach was used to evaluate the fit of the FFS-RF model (Meyer et al., 2018). The number of folds for cross-validation was set to five (Kuhn & Johnson, 2013) and the number of randomly selected independent variables to construct each tree was set to one-third of the number of independent variables (Breiman, 2001). The modeling process was implemented utilizing the package Caret in the R language (Williams et al. 2019, Meyer, 2018).

2.3.4. Land allocation using Cellular Automata

In this research, Cellular Automata (CA) was employed to implement a neighborhood effect when allocating the urban cells to simulate urbanization during 2018–2060. CA simulates spatiotemporal processes employing its four main components: 1 objects in any dimensional space, 2 the state of the object at a particular time point, 3 the neighborhood, and 4 transition rules (Batty, Couclelis, & Eichen 1997; Couclelis 1985). The most noticeable feature of the CA is transition rules, which can influence the simulation of temporal and spatial complexities. We employed a modified CA using non-stationary transition rules (Mirbagheri & Alimohammadi, 2017) because the synergy between urban growth and driving factors behaves differently in different locations (Luo & Wei 2009) and rules governing the land changes may alter in time and space (Santé, García, Miranda, & Crecente, 2010). The non-stationary transition rules were defined by the transition index derived from the calibrated FFS-RF model. Non-stationary transition rules are also in other studies (Feng, Wang, Tong, & Shafizadeh-Moghadam, 2019; Liu, 2009). Eq. (1) expresses the general concept of a cellular automata,

$$S^{t+1}{}_{ij} = f\left(S^{t}{}_{ij}, \Omega^{t}{}_{ij}, C, N\right) \tag{1}$$

where $S^{t+1}{}_{ij}$ is the state of cell ij at time t + 1, f is a transition function, $S^{t}{}_{ij}$ is the state of cell ij at time t, $\Omega^{t}{}_{ij}$ is a function of the neighborhood of cell ij at time t, C denotes the constraints, and N is the number of cells (Feng, Liu, Tong, Liu, & Deng, 2011). A kernel with a 5 × 5 window was used for dynamically calculating the neighborhood. The higher the TIM value and the more urban cells neighboring a given non-urban cell, the more chance the CA will allocate the cell as urban growth. The annual area during 2008–2018 was used to extrapolate the quantity of change during 2018–2060. The interval from 2008 to 2018 showed that 635,615 cells converted to urban, therefore, the size of urban growth during each of the following decades was 635,615 cells.

2.3.5. Evaluating the goodness-of-fit of transition index maps

We used the Total Operating Characteristic (TOC) to assess the TIMs in terms of the fit of calibration during 1998–2008 and validation during 2008–2018 using the R package by Pontius Jr, Santacruz, Tayyebi, and Parmentier (2015). The TOC is an improved version of the relative operating characteristic (ROC). The TOC compared a TIM to a map that shows urban growth versus non-urban persistence. The TOC considers a variety of thresholds for the TIM values in a sequence from largest to smallest. Each threshold generates Hits, Misses, False Alarms, and Correct Rejections. A Hit is a pixel of correctly simulated urban growth, a Miss is reference urban growth simulated as non-urban persistence, a False Alarm is reference non-urban persistence simulated as urban growth, and a Correct Rejection is correctly simulated non-urban persistence (Chen & Pontius Jr, 2010; Kamusoko & Gamba, 2015; Pontius Jr et al., 2018). The sum of Misses and False alarms equals the error whereas the sum of Hits and Correct Rejections equals the agreement (Feng et al., 2019). In each TOC, the non-urban at the start time is the maximum value on the horizontal axis and the size of urban growth during the time interval is the maximum value on the vertical axis. Each threshold produces a point on the TOC curve, which has a horizontal coordinate corresponding to the size of the simulated urban growth and a vertical coordinate corresponding to the size of Hits. The maximum and minimum dashed lines form a parallelogram that defines the possible space for the TOC curve. The TOC delivers results in terms of area along the axes and in terms of intensity as the slope of the segments of the curve, e.g. additional Hit area per additional simulated urban growth area. Pontius Jr and Si (2014) gives more details regarding TOC.

3. Results

3.1. Data exploration

Fig. 7 is the network plot that shows the correlation between pairs of driving forces of urban growth. Green connections indicate positive correlations and red connections indicate negative correlations. The strongest correlation during 1998–2008 was between distance from roads and distance from urban, as well as between slope and altitude. Slope and altitude are highly correlated during 1998–2008 and 2008–2018. The distance from road, distance from urban, and distance from crop also show strong correlations. These relationships notify the importance of the coupling feature selection in this study because several independent variables convey a high degree of redundant information.

Fig. 8 shows the urban growth during 1998–2008 and 2008–2018 concerning the independent variables at 1998 and 2008, respectively. The urban growth was mostly concentrated in lower altitudes and lower slopes during the first interval, then the urban growth shifted towards higher altitudes during the second interval. The urban growth is intensive near green spaces during the first time interval then shifts to farther distances during the second time interval. Comparatively, the urban growth during the second time interval is found around the already urban areas. Both intervals experience urban growth nearer to the roads and crops.

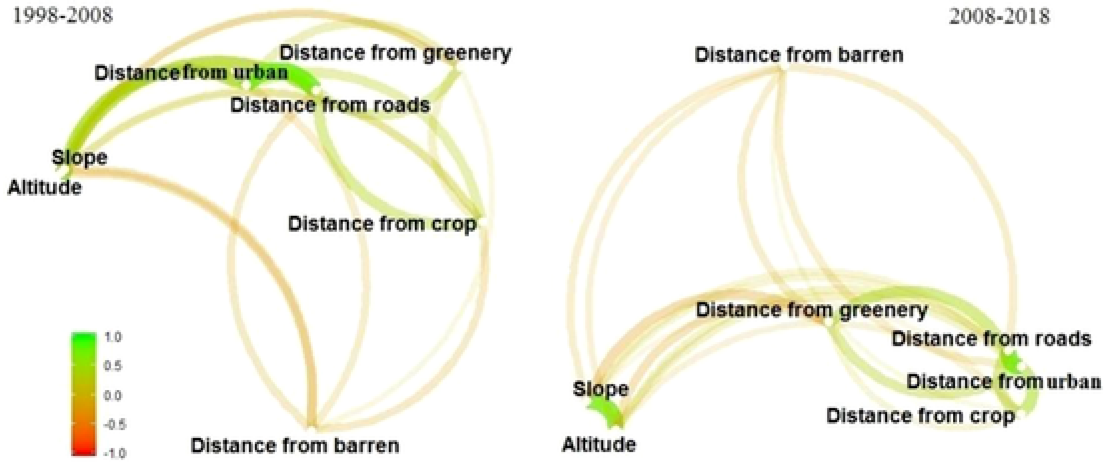

Fig. 7. Network plot to visualize correlations between pairs of independent variables during 1998–2008 and 2008–2018.

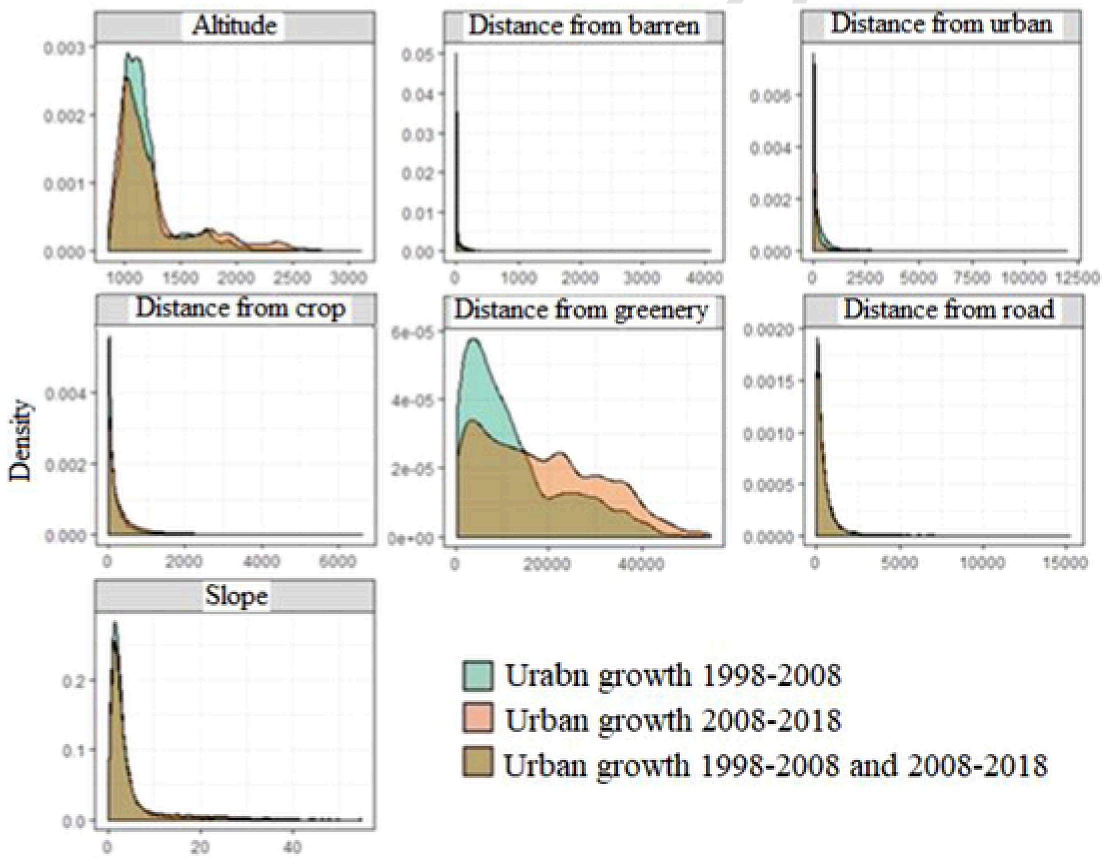

Fig. 8. The urban growth during 1998–2008 and 2008–2018 as a function of the independent variables at 1998 and 2008, respectively.

3.2. Behavior of the FFS-RF model

The FFS-RF iterates based on the sequential inclusion of independent variables. Fig. 9a and c show the results of this process where the horizontal axis shows the number of model iterations and the vertical axis indicates the accuracy of the fit. The modeling process was carried out 36 iterations for the calibration during 1998–2008 and 26 iterations for the detection during 2008–2018. Fig. 9a shows that six independent variables produce the best fit while the addition of the seventh variable decreases the fit, thus Fig. 9b shows six variables. Fig. 8c shows that the inclusion of a third variable does not increase fit substantially during 2008–2018, therefore Fig. 8d shows two variables. Fig. 9b shows that during 1998–2008 the variables' order of importance is: distance from greenery, altitude, and distance from crop, urban, road, and barren. Fig. 9d shows that during 2008–2018, the variables' order of importance is the distance from crop and barren. The remaining independent variables were excluded as either negligible or counterproductive (Ludwig et al., 2019).

3.3. Transition Index Maps

One of the intermediate results of urban growth simulation models is the TIM. The TIM gives each pixel a relative index for urban growth

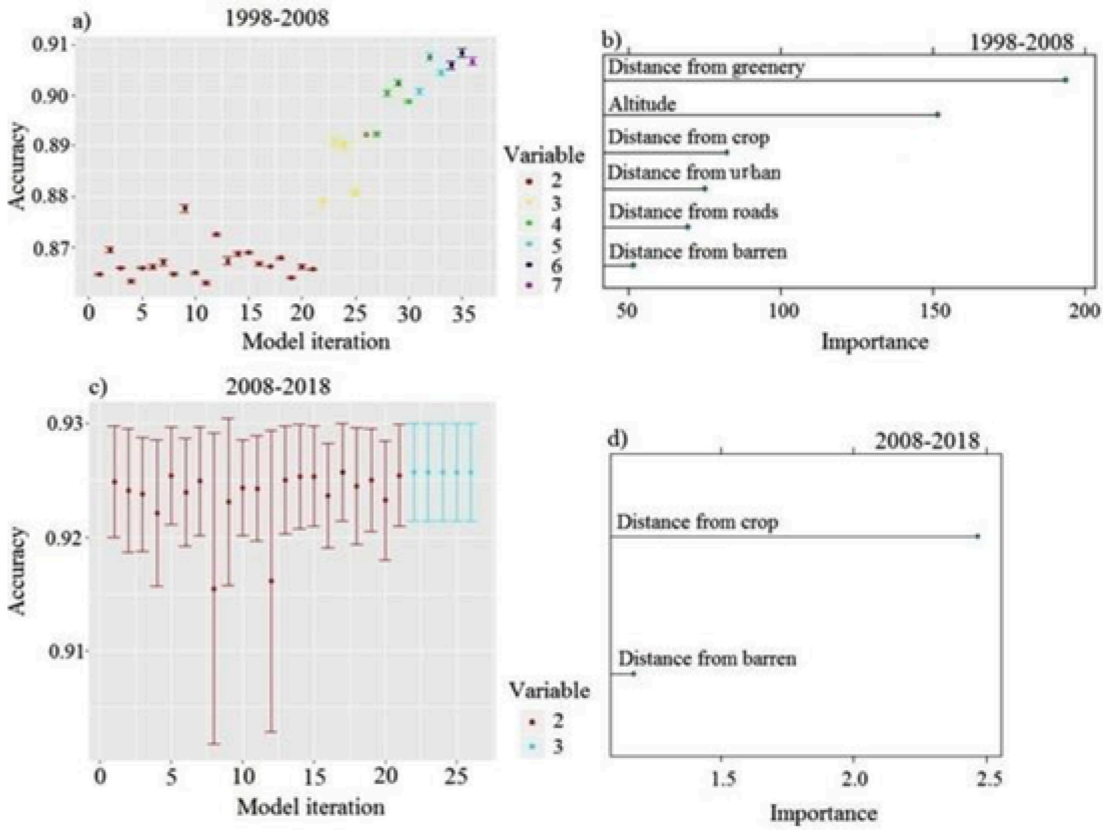

Fig. 9. a) Goodness-of-fit of the FFS-RF model during 1998–2008 calibration, b) the relative importance of variables during 1998–2008, c) goodness-of-fit during 2008–2018 detection, and d) the relative importance of variables during 2008–2018.

using a continuous range of values from 0 indicating no potential to 1 indicating the full potential of urban growth. Fig. 10a shows the TIM to extrapolate urban growth between 2008 and 2018. Fig. 10b shows the TIM to extrapolate urban growth beyond 2018. The earlier derives from independent variables at 2008, and the latter derives from independent variables at 2018. Most of the suitable regions are located in the south of the study area, particularly in the south of Tehran and Karaj, and southwest of Tehran. Another striking patch is Lavasan, situated 11 km northeast of Tehran, which has witnessed widespread construction during recent years. Fig. 9b shows that Lavasan has relatively high potential, hence the future extrapolation concentrates the urban growth near Lavasan. A very high index is also observed between Tehran and Karaj and between other cities in the region such as Pakdasht, Varamin, Eslamshahr, Robatkarim, Shahr-e-Rey, and Shahriar. High-ranking TIM values exist southeast of Tehran, including Varamin, Qarechak, Pakdasht, and Pishva. The towns surrounding the south and southeast of Karaj such as Mahdasht, Mohammadshahr, Malard, Andisheh, and Qods also show relatively high growth potential. Karaj-Hashtgerd in northwest Karaj has substantial potential for growth, though it is much lower than in south Karaj. Both maps show that the distance from urban is associated with the highest growth potential. The TIMs show also the effect of the distance from roads.

3.4. The goodness of fit using the Total operating characteristic

Fig. 11 shows the TOC curves for (a) calibration during 1998–2008 and (b) validation during 2008–2018. Maps of distance from urban areas at 2008 and 2018 were considered as TIMs and evaluated using the TOC to establish a baseline for comparison to the FFS-RF models. The maximum value on the horizontal axis in Fig. 11a and b is the size of non-urban at 1998 and 2008, respectively. The size of urban growth during 1998–2008 and 2008–2018 is 1084 and 573 square km respectively, thus those are the maximum values on the vertical axes. The upper left corner of the TOC parallelogram has a horizontal coordinate that matches the size of the reference urban growth. The point on the TOC curve at that horizontal coordinate indicates that the sum of Misses and False Alarms is 3.4 times larger than Hits for the validation of both FFS-RF and the Baseline. The Area Under the Curve (AUC) is 92% and 82% respectively for the FFS-RF and the Baseline for the calibration during 1998–2008. The AUC is 81% and 82% respectively for the FFS-RF and the Baseline for the validation during 1998–2008. The validation curves are nearly identical for FFS-RF and Baseline. Fig. 12 superimposes the reference maps at 2008 and 2018 with the simulated map at 2018 where the quantity of simulated change equals the quantity of reference change. The three-map comparison reveals the spatial distribution of Hits, Misses, False Alarms, and Correct Rejections. Hits and False Alarms are near the urban at 2008. The simulation missed the urban growth that was farther from urban at 2008.

3.5. Simulating the future pattern of the Tehran-Karaj Region (TKR)

Fig. 13 shows the simulated urbanization from 2018 to 2060. The TIMs cause the simulated maps to extrapolate urban from cropland in the south. Simulated maps show that cropland shrink by 80% by 2060. Tehran, Karaj, and other surrounding cities become spatially interconnected. Tehran's counties experience widespread growth towards the south and southeast, in counties such as Pakdasht, Varamin, Eslamshahr, Robatkarim, Shahr-e-Rey, and Shahriar, Qarechak, and Pakdasht. Lavasan expands considerably. Northwest Karaj also grows in Nazarabad and Hashtgerd. The urban expansion continues in the high altitudes north and east of Tehran.

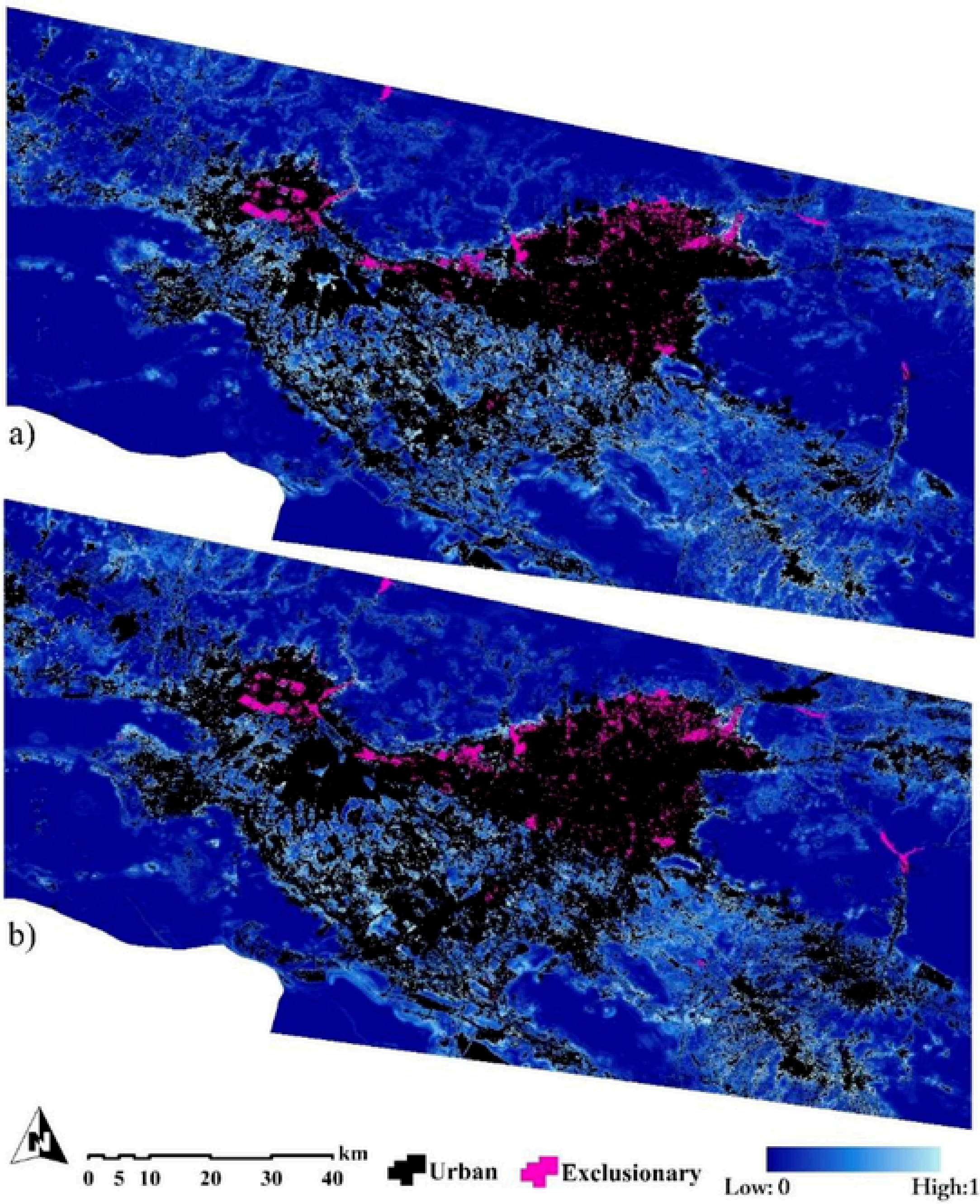

Fig. 10. Transition Index Maps showing (a) the potential of urban growth during 2008–2018 based on variables at 2008, and (b) the potential of urban growth after 2018 based on variables at 2018. The magenta color indicates the exclusionary zone where no urban growth occurs due to limitations including greenery and water. Readers of the black & white paper version of this article should access the digital version to see the colors.

4. Discussion

4.1. Monitoring urban growth in the TKR

Scientists have conducted extensive urban agglomeration studies in North America (Hajrasouliha and Hamidi 2017), Europe (Krehl & Siedentop, 2019; Salvati & Gargiulo Morelli, 2014), and East Asia (He et al. 2019), but less attention has been paid to emerging urban agglomerations in West Asia, specifically Iran's capital, Tehran. Growth around Tehran emerged in many ways, such as the expansion of surrounding cities, the conversion of villages to cities, and the creation of cities. Consequently, urban centers around Tehran expanded rapidly. The economic, social, and physical relationships between Tehran and neighboring cities entered a new phase that eventually led to the formation of an emerging urban agglomeration.

Monitoring urbanization in the TKR showed that urban growth during the first interval, 1998–2008, was approximately twice that during the second interval, 2008–2018. Our understanding of the study area and historical context of the driving forces guided us to select the latter time interval to extrapolate the amount of change in the future. Growth during 2008–2018 was 573 km^2 per decade, thus the extrapolation beyond 2018 assumes an increase in the urban area of 57.3 km^2 per year. We allocated the annual number of pixels by using the transition index map and the CA model.

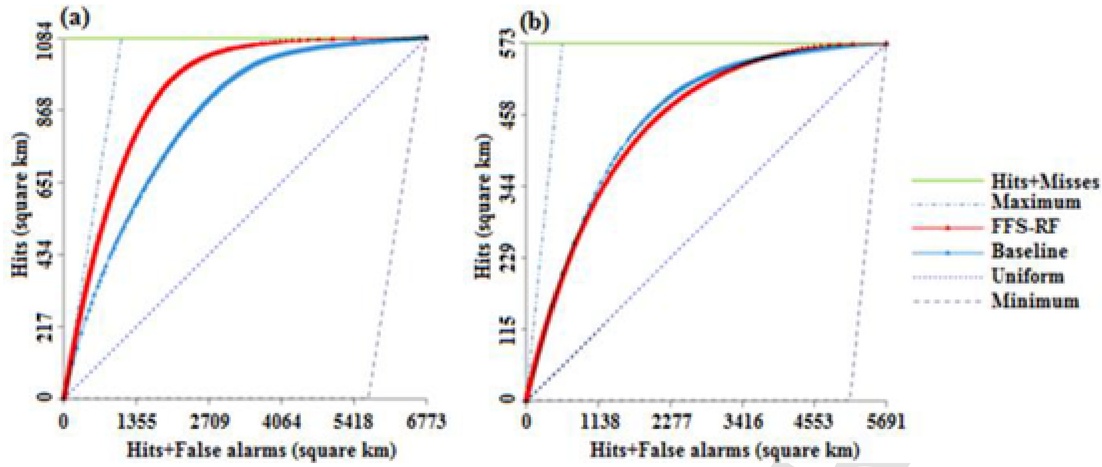

Fig. 11. Total Operating Characteristic for evaluation of urban growth for (a) FFS-RF calibration during 1998–2008 and distance from urban at 1998, and (b) FFS-RF validation during 2008–2018 and distance from urban at 2008.

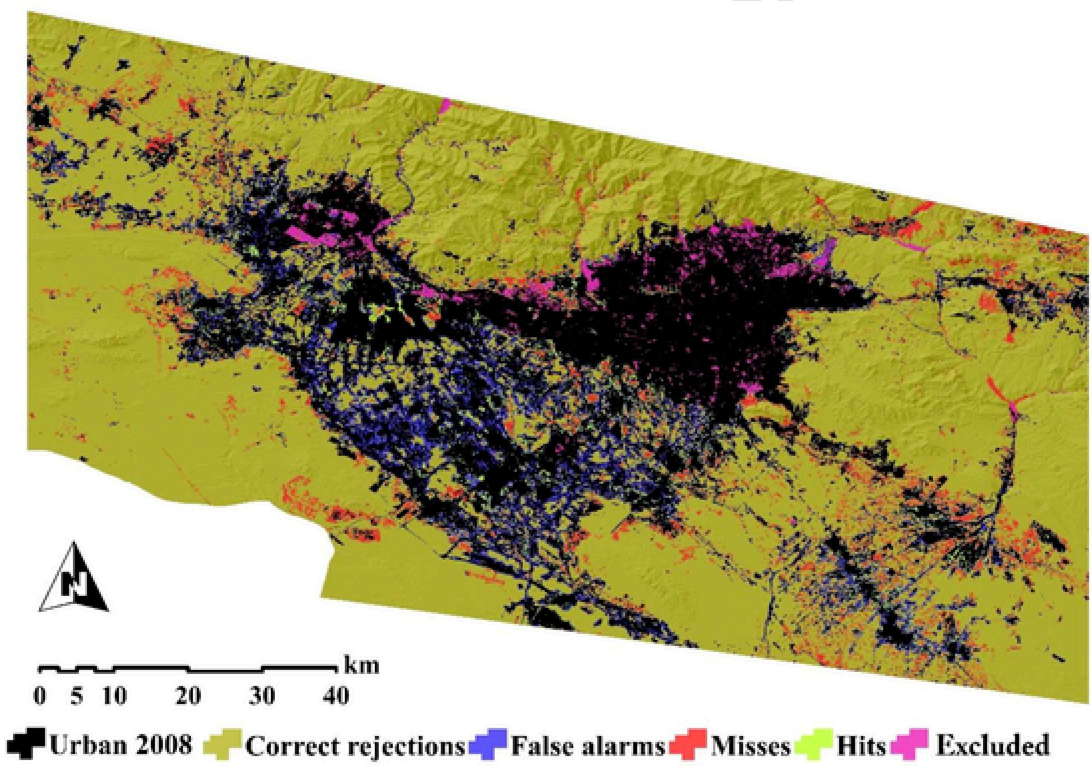

Fig. 12. The map of accuracy and error by superimposing the reference maps at 2008 and 2018 with the simulated map at 2018.

4.2. Temporal evaluation of driving forces of urban growth in the TKR

The spatiotemporal process of urban growth in the TKR is a product of continuous dynamics of centralized and decentralized forces and is produced and reproduced across various time intervals, due to the strength or weakness of the influencing factors. These forces during any given time interval have influenced the process of urban growth in Tehran's urban agglomeration either due to general principles and regulations such as the principle of economies of scale and agglomeration, or driven by incentives in the form of policies, plans, and programs. Driving forces come with the complex interactions between the social and biophysical features of the region. Previous studies explored the local operation and spatial non-stationary of urban growth drivers (Mirbagheri & Alimohammadi, 2017; Shafizadeh-Moghadam & Helbich, 2015). Our paper investigated the temporal effect of some factors that affected urbanization during 1998–2008 and 2008–2018.

One of the advantages of using the RF algorithm is the ranking of the independent variables to explain urban growth. Fig. 9 shows that the most important variables during the first time interval were in sequence of importance: distance from greenery, altitude, distance from crop, distance from urban, distance from road, and distance from barren. The slope was not an important independent variable during the first time interval. Fig. 8 shows that urbanization is relatively more dense closer to greenery and on lower altitudes. During the second time interval, the most important factors of urban growth were only distance from crop and distance from barren. This shows there is not a stable relationship between urban growth over time and the detailed driving

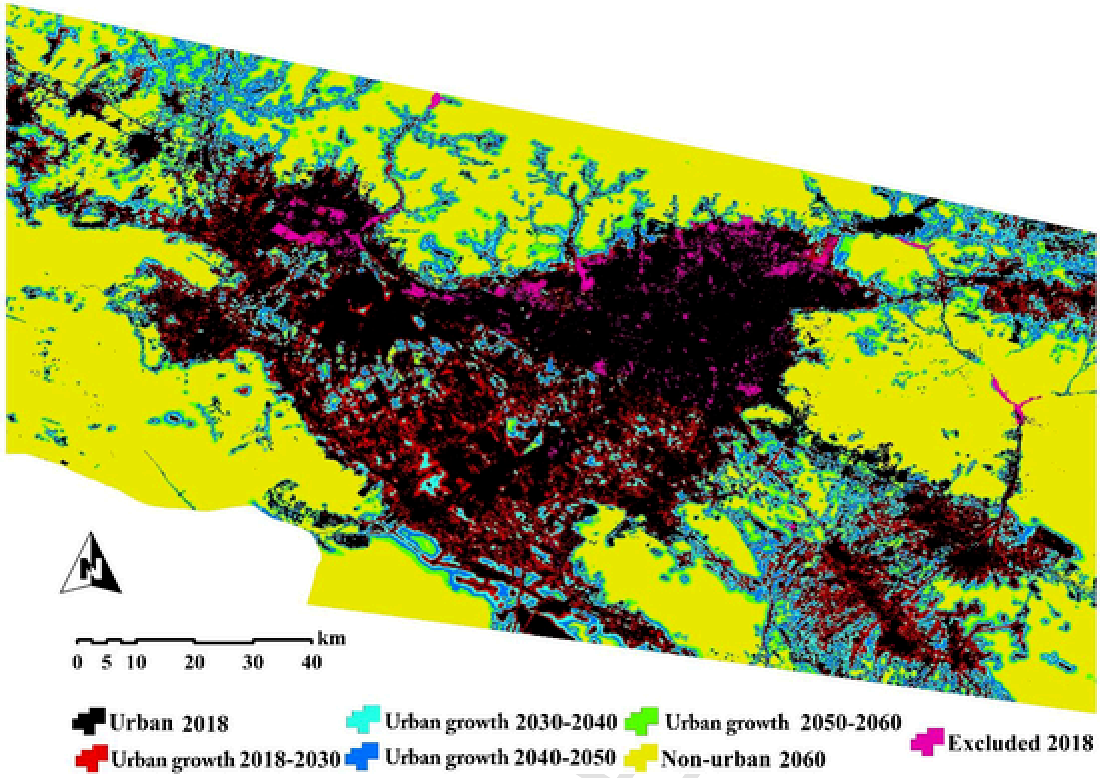

Fig. 13. Urban growth simulation in the Tehran-Karaj Region from 2018 to 2060.

forces that FFS-RF finds. Results of feature selection during 2008–2018 are consistent with the field observations that construction has occurred relatively more intensively where barren land was available. Riversides, hilly areas, and tops of mountains are among the places that have been intensively constructed during recent years. On the other hand, crops and gardens have exponentially disappeared in favor of extensive constructions. For example, Karaj was previously known for its extensive gardens and favorable climate, but now, a large portion of previous gardens are urban. These results are confirmed by the land use map (Fig. 3) and urban growth map (Fig. 4), where urban growth during 1998–2008 showed a pattern of infill, but during 2008–2018 showed a pattern of expansion to the south and east of Tehran, also between Tehran and Karaj. Our results are in line with previous studies that high-quality croplands around cities are consumed by urban expansion (d'Amour et al., 2017; Jiang, Deng, & Seto, 2013; Liu et al., 2019; Song, Pijanowski, & Tayyebi, 2015).

4.3. FFS-RF compared to a baseline model

Fig. 11a shows that the FFS-RF model has a slightly better fit to the calibration data than the baseline model of proximity. This means that the FFS-RF discovered variables that have a better fit to the calibration data during 1998–2008 than a baseline fit of the distance from 1998 urban. However, Fig. 9 shows the detailed pattern that the FFS-RF detected during 1998–2008 did not continue into the subsequent time interval. Therefore, Fig. 11b shows that the FFS-RF model calibrated during 1998–2008 has predictive power not greater than a baseline model of distance from urban at 2008. Urban expansion occurred near the existing urbanized areas during both time intervals. Consequently, a prediction that urban will grow near the existing urbanized areas has predictive power slightly greater than the FFS-RF model. In short, the FFS-RF model detected ephemeral details, thus has predictive power no better than a much simpler model that assumes future urbanization will continue to grow near previous urban. Other applications of land change modeling have found similar results, meaning a simple baseline model has greater predictive power than a more complex model (Pontius Jr et al., 2007). Most of the papers we found in the literature never compare a simple baseline model to the more complex model that the paper endorses. The baseline model has a larger AUC than the FFS-RF model during the validation interval, which is one decade. However, the extrapolation extends beyond four decades, which means the extrapolation extends into outlying areas (Wilson, Hurd, Civco, Prisloe, & Arnold, 2003). The FFS-RF distinguishes among the various characteristics of areas that are far from the urban at 2018, which are characteristics that the baseline model does not distinguish.

4.4. Considerations of urban growth in the TKR

The expansion of TKR has always been accompanied by the continuous influx of population into the peripheral areas and loss of open and natural spaces. The TKR lacks an efficient and integrated mechanism for controlling urban agglomeration expansion. The natural environment around this region has witnessed environmental degradation, widespread change of agricultural and natural environments, and intensification of types of speculative intrusions and uncontrolled construction (Dadashpoor, Azizi, & Moghadasi, 2019; Daneshpour & Tarantash, 2017; Ghamami, Khatam, Atahari, & Offsar, 2007; Minaei, Shafizadeh-Moghadam, & Tayyebi, 2018). Due to the massive scale and speed of urbanization, the environmental problems in the cities of developing countries are much greater than elsewhere (Atash, 2007). For example, over-concentration of economic activities and people, as well as an increasing vehicle fleet has led to air pollution in cities like Tehran (Atash, 2007). Extrapolation during 2018–2060 shows an urban increase of 2.4 thousand square kilometers. If recent trends continue through 2060, then these problems will be intensified in the future considering the emergence of interconnected urban areas in the TKR according to the simulated map. Urban planners and decision-makers would have to make bold decisions soon if they want to avoid the current trajectory.

5. Conclusion

This article integrated a forward feature selection (FFS) algorithm with the Random Forest (RF) model to examine the driving forces of urban growth during 1998–2008 and 2008–2018, and then to extrapolate the growth pattern during 2018–2060 in the TKR, which is an emerging urban agglomeration area in Iran. The independent variables that FFS-RF selected during the first time interval were different from the independent variables during the second time interval, implying that the FFS-RF found non-stationary urban growth drivers through time. For comparison to the FFS-RF, a baseline model assumed urban growth occurs simply near the urban at the start of each time interval. TOC validation through time shows that the predictive power of the FFS-RF model is no better than a baseline model of an urban expansion near the existing urban. This demonstrates how the distance to the existing urban areas can be a desirable approach for simulating urban growth, especially for regions that lack data concerning the variety of possible driving forces. One of our limitations is the lack of socio-economic data and master plans. It is not clear whether such data would have increased the predictive accuracy of the FFS-RF. An important lesson of our article is that modelers should always compare a sophisticated model to a baseline model during extrapolation through a validation time interval that extends beyond the calibration time interval.

Our model's extrapolation shows that the TKR becomes a gigantic interconnected urban entity by 2060. The model assumes that the recent driving forces of urban growth will continue during the coming decades. However, driving forces and their importance have changed over time and can change again in the future. Thus, policymakers must appreciate that decisions today can modify trajectories so to attain a future that is more desirable than the model's extrapolation of recent trends.

Funding

The United States National Science Foundation supported this work through its Long Term Ecological Research Network via grant OCE-1637630 for Plum Island Ecosystems.

Classifications

10: Urban Modeling
40: Urban Growth
140: Geographic Information Systems
150: Land Use Change
550: Land Use Modeling
1180: Land Cover Change

Uncited reference

Declaration of competing interest

The authors report no conflicts of interest.

References

Atash, F. (2007). The deterioration of urban environments in developing countries: Mitigating the air pollution crisis in Tehran, Iran. Cities, 24(6), 399–409. doi:10.1016/j.cities.2007.04.001.

Breiman, L. (2001). Random forests. Machine Learning, 45(1), 5–32. doi:10.1023/a:1010933404324.

Brennan, L.A., Tri, A.N., & Marcot, B.G. (eds.). (2019). Quantitative analyses in wildlife science. Baltimore: Johns Hopkins University Press.

Chen, H., & Pontius, R.G., Jr. (2010). Diagnostic tools to evaluate a spatial land change projection along a gradient of an explanatory variable. Landscape Ecology, 25(9), 1319–1331. doi:10.1007/s10980-010-9519-5.

Dadashpoor, H., Azizi, P., & Moghadasi, M. (2019). Analyzing spatial patterns, driving forces and predicting future growth scenarios for supporting sustainable urban growth: Evidence from Tabriz metropolitan area, Iran. Sustainable Cities and Society, 47, 101502. doi:10.1016/j.scs.2019.101502.

d'Amour, C.B., Reitsma, F., Baiocchi, G., Barthel, S., Güneralp, B., Erb, K.H., … Seto, K.C. (2017). Future urban land expansion and implications for global croplands. Proceedings of the National Academy of Sciences, 114(34), 8939–8944. doi:10.1073/pnas.1606036114.

Daneshpour, Z., & Tarantash, M. (2017). Revealing land-use transformation: Analysing specifications of unplanned growth in the metropolitan region of Tehran. Honar-Ha-ye-Ziba, 22, 15–32.

Fang, C., & Yu, D. (2017). Urban agglomeration: An evolving concept of an emerging phenomenon. Landscape and Urban Planning, 162, 126–136. doi:10.1016/j.landurbplan.2017.02.014.

Fanni, Z. (2006). Cities and urbanization in Iran after the Islamic revolution. Cities, 23(6), 407–411. doi:10.1016/j.cities.2006.08.003.

Feng, Y., Liu, Y., & Liu, Y. (2017). Spatially explicit assessment of land ecological security with spatial variables and logistic regression modeling in Shanghai, China. Stochastic Environmental Research and Risk Assessment, 31(9), 2235–2249. doi:10.1007/s00477-016-1330-7.

Feng, Y., Liu, Y., Tong, X., Liu, M., & Deng, S. (2011). Modelling dynamic urban growth using cellular automata and particle swarm optimization rules. Landscape and Urban Planning, 102(3), 188–192. doi:10.1016/j.landurbplan.2011.04.004.

Feng, Y., Wang, R., Tong, X., & Shafizadeh-Moghadam, H. (2019). How much can temporally stationary factors explain cellular automata-based simulations of past and future urban growth? Computers, Environment and Urban Systems, 76, 150–162. doi:10.1016/j.compenvurbsys.2019.04.010.

Geddes, P.S. (1915). Cities in evolution: An introduction to the town-planning movement and the study of cities. London: Williams.

Ghamami, M., Khatam, A., Atahari, K., & Offsar, R. (2007). Integrated management and problem-solving of informal settlements: Conditions for realization of Tehran urban agglomeration. Tehran: Shahidi Publications.

Gounaridis, D., Chorianopoulos, I., Symeonakis, E., & Koukoulas, S. (2019). A Random Forest-Cellular Automata modelling approach to explore future land use/cover change in Attica (Greece), under different socio-economic realities and scales. Science of the Total Environment, 646, 320–335. doi:10.1016/j.scitotenv.2018.07.302.

Habibi, M., & Horcad, B. (2005). Atlas of Tehran Metropolis. Tehran: Urban Planning and Processing Organization.

Howard, E. (1902). Garden cities of to-morrow: Being the second edition of "Tomorrow: A peaceful path to real reform". London: Swan Sonnenschein & Co. Cambridge, MA, MIT Press.

Hu, Z., & Lo, C.P. (2007). Modeling urban growth in Atlanta using logistic regression. Computers, Environment and Urban Systems, 31(6), 667–688. doi:10.1016/j.compenvurbsys.2006.11.001.

Jiang, L., Deng, X., & Seto, K.C. (2013). The impact of urban expansion on agricultural land use intensity in China. Land Use Policy, 35, 33–39. doi:10.1016/j.landusepol.2013.04.011.

Kamusoko, C., & Gamba, J. (2015). Simulating urban growth using a random forest-cellular automata (RF-CA) model. ISPRS International Journal of Geo-Information, 4(2), 447–470. doi:10.3390/ijgi4020447.

Krehl, A., & Siedentop, S. (2019). Towards a typology of urban centers and subcenters–evidence from German city regions. Urban Geography, 40(1), 58–82. doi:10.1080/02723638.2018.1500245.

Kuhn, M., & Johnson, K. (2013). Applied predictive modeling. New York: Springer.

Lin, Y.P., Chu, H.J., Wu, C.F., & Verburg, P.H. (2011). Predictive ability of logistic regression, auto-logistic regression and neural network models in empirical land-use change modeling–a case study. International Journal of Geographical Information Science, 25(1), 65–87. doi:10.1080/13658811003752332.

Liu, F., Zhang, Z., Zhao, X., Wang, X., Zuo, L., Wen, Q., … Liu, B. (2019). Chinese cropland losses due to urban expansion in the past four decades. Science of the Total Environment, 650, 847–857. doi:10.1016/j.scitotenv.2018.09.091.

Liu, Y.O. (2009). Modelling urban development with geographical information systems and cellular automata. Boca Raton, Fla, London: CRC Press.

Ludwig, M., Morgenthal, T., Detsch, F., Higginbottom, T.P., Valdes, M.L., Nauß, T., & Meyer, H. (2019). Machine learning and multi-sensor based modelling of woody vegetation in the Molopo Area, South Africa. Remote Sensing of Environment, 222, 195–203. doi:10.1016/j.rse.2018.12.019.

Meyer, H. (2018). CAST: "Caret" applications for spatial-temporal models, R Package Version 0.1. 0.

Meyer, H., Reudenbach, C., Hengl, T., Katurji, M., & Nauss, T. (2018). Improving performance of spatio-temporal machine learning models using forward feature selection and target-oriented validation. Environmental Modelling & Software, 101, 1–9. doi:10.1016/j.envsoft.2017.12.001.

Minaei, M., & Kainz, W. (2016). Watershed land cover/land use mapping using remote sensing and data mining in Gorganrood, Iran. ISPRS International Journal of Geo-Information, 5(5), 57. doi:10.3390/ijgi5050057.

Minaei, M., Shafizadeh-Moghadam, H., & Tayyebi, A. (2018). Spatiotemporal nexus between the pattern of land degradation and land cover dynamics in Iran. Land Degradation & Development, 29(9), 2854–2863. doi:10.1002/ldr.3007.

Mirbagheri, B., & Alimohammadi, A. (2017). Improving urban cellular automata performance by integrating global and geographically weighted logistic regression models. Transactions in GIS, 21(6), 1280–1297. doi:10.1111/tgis.12278.

Moulds, S., Buytaert, W., & Mijic, A. (2015). An open and extensible framework for spatially explicit land use change modelling: The lulcc R package. Geoscientific Model Development, 8, 3215–3229. doi:10.5194/gmd-8-3215-2015.

Paegelow, M., Camacho Olmedo, M.T., Houet, T., Mas, J.-F., & Pontius, R.G., Jr. (2013). Land change modeling: Moving beyond projections. International Journal of Geographical Information Science, 27(9), 1691–1695.

Pijanowski, B.C., Brown, D.G., Shellito, B.A., & Manik, G.A. (2002). Using neural networks and GIS to forecast land use changes: A land transformation model. Computers, Environment and Urban Systems, 26(6), 553–575. doi:10.1016/s0198-9715(01)00015-1.

Pontius, R.G., Jr., Castella, J.-C., de Nijs, T., Duan, Z., Fotsing, E., Goldstein, N., … Veldkamp, A.T. (2018). Lessons and challenges in land change modeling derived from synthesis of cross-case comparisons. In Behnisch, M., & Meinel, G. (Eds.), Trends in spatial analysis and modelling (19, pp. 143–164). Springer International Publishing. doi:10.1007/978-3-319-52522-8_8.

R.G. Pontius Jr. A. Santacruz A. Tayyebi B. Parmentier TOC: Total operating characteristic curve and ROC curve (version 0.0-4) [R]https://cran.r-project.org/web/packages/TOC2015

Pontius, R.G., Jr., & Si, K. (2014). The total operating characteristic to measure diagnostic ability for multiple thresholds. International Journal of Geographical Information Science, 28(3), 570–583. doi:10.1080/13658816.2013.862623.

Pontius, R.G., Jr., Walker, R., Yao-Kumah, R., Arima, E., Aldrich, S., Caldas, M., & Vergara, D. (2007). Accuracy assessment for a simulation model of Amazonian deforestation. Annals of the Association of American Geographers, 97(4), 677–695. doi:10.1111/j.1467-8306.2007.00577.x.

Rafiee, R., Mahiny, A.S., Khorasani, N., Darvishsefat, A.A., & Danekar, A. (2009). Simulating urban growth in Mashad City, Iran through the SLEUTH model (UGM). Cities, 26(1), 19–26. doi:10.1016/j.cities.2008.11.005.

Rienow, A., & Goetzke, R. (2015). Supporting SLEUTH–enhancing a cellular automaton with support vector machines for urban growth modeling. Computers, Environment and Urban Systems, 49, 66–81. doi:10.1016/j.compenvurbsys.2014.05.001.

Salvati, L., & Gargiulo Morelli, V. (2014). Unveiling urban sprawl in the Mediterranean region: Towards a latent urban transformation? International Journal of Urban and Regional Research, 38(6), 1935–1953. doi:10.1111/1468-2427.12135.

Santé, I., García, A.M., Miranda, D., & Crecente, R. (2010). Cellular automata models for the simulation of real-world urban processes: A review and analysis. Landscape and Urban Planning, 96(2), 108–122. doi:10.1016/j.landurbplan.2010.03.001.

Shafizadeh-Moghadam, H. (2019). Improving spatial accuracy of urban growth simulation models using ensemble forecasting approaches. Computers, Environment and Urban Systems, 76, 91–100. doi:10.1016/j.compenvurbsys.2019.04.005.

Shafizadeh-Moghadam, H., Asghari, A., Tayyebi, A., & Taleai, M. (2017). Coupling machine learning, tree-based and statistical models with cellular automata to simulate urban growth. Computers, Environment and Urban Systems, 64, 297–308. doi:10.1016/j.compenvurbsys.2017.04.002.

Shafizadeh-Moghadam, H., Hagenauer, J., Farajzadeh, M., & Helbich, M. (2015). Performance analysis of radial basis function networks and multi-layer perceptron networks in modeling urban change: A case study. International Journal of Geographical Information Science, 29(4), 606–623. doi:10.1080/13658816.2014.993989.

Shafizadeh-Moghadam, H., & Helbich, M. (2015). Spatiotemporal variability of urban growth factors: A global and local perspective on the megacity of Mumbai. International Journal of Applied Earth Observation and Geoinformation, 35, 187–198. doi:10.1016/j.jag.2014.08.013.

Song, W., Pijanowski, B.C., & Tayyebi, A. (2015). Urban expansion and its consumption of high-quality farmland in Beijing, China. Ecological Indicators, 54, 60–70. doi:10.1016/j.ecolind.2015.02.015.

Statistical Center of Iran https://www.amar.org.ir/2016accessed 02/01/2020

Tayyebi, A., & Pijanowski, B.C. (2014). Modeling multiple land use changes using ANN, CART and MARS: Comparing tradeoffs in goodness of fit and explanatory power of data mining tools. International Journal of Applied Earth Observation and Geoinformation, 28, 102–116. doi:10.1016/j.jag.2013.11.008.

Valavi, R., Elith, J., Lahoz-Monfort, J.J., & Guillera-Arroita, G. (2018). BlockCV: an R package for generating spatially or environmentally separated folds for k-fold cross-validation of species distribution models. bioRxiv. doi:10.1111/2041-210x.13107. 357798.

Wang, R., Derdouri, A., & Murayama, Y. (2018). Spatiotemporal simulation of future land use/cover change scenarios in the Tokyo metropolitan area. Sustainability, 10(6), 2056. doi:10.3390/su10062056.

Wei, C., Taubenböck, H., & Blaschke, T. (2017). Measuring urban agglomeration using a city-scale dasymetric population map: A study in the Pearl River Delta, China. Habitat International, 59, 32–43. doi:10.1016/j.habitatint.2016.11.007.

Wilson, E.H., Hurd, J.D., Civco, D.L., Prisloe, M.P., & Arnold, C. (2003). Development of a geospatial model to quantify, describe and map urban growth. Remote Sensing of Environment, 86(3), 275–285. doi:10.1016/S0034-4257(03)00074-9.

Zhang, Z., Wang, B., Buyantuev, A., He, X., Gao, W., Wang, Y., & Yang, Z. (2019). Urban agglomeration of Kunming and Yuxi cities in Yunnan, China: The relative importance of government policy drivers and environmental constraints. Landscape Ecology, 34(3), 663–679. doi:10.1007/s10980-019-00790-2.

Zhou, S., Huang, Y., Yu, B., & Wang, G. (2015). Effects of human activities on the eco-environment in the middle Heihe River Basin based on an extended environmental Kuznets curve model. Ecological Engineering, 76, 14–26. doi:10.1016/j.ecoleng.2014.04.020.